

A REPRESENTATION OF LOCAL REALISM

1.1 BACKGROUND

QuWT-c1-220417

There are several impediments to the formulation of a locally real representation of quantum mechanics. However, by far the most notable is the perceived exclusion of “locally real hidden variable theories” (HVT) based upon results of performed experiments in conjunction with Bell’s Theorem. [329]

In that regard, the particular LR representation of local realism [102]-C derived from first principles of the underlying quantum formalism is shown to be in exact agreement with the standard Probabilistic Interpretation of quantum mechanics (PI) and in agreement with results of performed experiments. The LR representation is inherently inclusive of a 3-dimensional wave structure for photons and an analogous 3-dimensional wave structure for particles. Based on the parameters of those wave structures, LR is appropriately categorized as a locally real hidden variable theory, HVT.

For example, in LR the objectively real longitudinal aspect of photon wave structure (along the propagation axis) is represented by the wave function of the underlying quantum mechanical formalism. However, critically with respect to hidden variables, that longitudinal aspect is shown to span an arc in the transverse plane. For any given photon, the magnitude of the arc span and the orientation of the arc bisector are appropriately regarded as the hidden variables attributable to that photon. For virtually all commonly generated photons, the magnitude of that arc span is a “full complement” $\Delta = \pi/2$. The arc bisector orientation θ fully determines the measurement outcome of that photon traversing a polarizer for which the polarization axis is specified.

Notably, however, for correlated pairs of photons (as well as for correlated pairs of particles) there is a naturally occurring asymmetry of the wave structures of the pair members. For photons, this asymmetry is manifested by one pair member, the “generator” photon, having a full complement $\Delta_G = \pi/2$ arc span while the “emission” photon it produces has an arc span $\Delta_E \leq \pi/2$ that ranges from 0 to $\pi/2$. The particular Δ_E value for any correlated

photon pair is that of a random member of a well-defined emission ensemble of photons. The average arc span of the emission ensemble members is approximately $2/3$ of $\pi/2$ and the emission photons are characterized as having a partial complement arc span. Additionally, the generator photon and the emission photon arcs of every pair of correlated photons have aligned bisectors and those arcs can be conveniently represented with a common orientation on a single reference frame.

Because of the partial complement arc span of the emission member, a “correlated” pair of generator and emission photons results in the characteristic quantum mechanical joint polarizer sampling result of $\cos^2 \theta$. In contrast, a pair of photons extracted from a single mode of a coherent beam are fully symmetric and identical in every sense including a common bisector orientation and a common full complement arc span. When such pairs are subjected to a joint polarizer sampling the result is a linear $1-2\theta/\pi$. These symmetric pairs are certainly also correlated but less so than the asymmetric generator-emission pairs.

From the perspective of LR, asymmetric and symmetric pairs both exhibit mathematical correlation levels that are directly attributable to their respective objectively real structures. In the explicit PI exclusion of objectively real structures, the term “correlated” elevates entities so designated as non-classically entangled.

Finally, it is important to review the relationship of LR to Bell’s Theorem. A consequence of the asymmetry of the generator-emission pairs is that ultra-correlated members exhibit the property of “enhancement” when measured. In the context of photons, enhancement means that the transmission of an objectively real fully specified photon through a randomly oriented polarizer is enhanced by transmitting that photon through a second, specified polarizer. A full complement photon, such as a generator photon, has a 50% probability of being transmitted through a randomly oriented polarizer whereas for an average emission photon that probability drops to $\sim(2/3)50\%$. However, if a specified emission photon is transmitted through a specified polarizer (oriented to ensure transmission of the specified emission photon), that emission photon emerges as a full complement $\Delta=\pi/2$ arc span photon with a subsequent transmission probability through a randomly oriented polarizer of 50%. As a result, transmission of the emission photon member

of an ultra-correlated pair through a polarizer enhances that photon's transmission probability through a randomly oriented polarizer. A similar analysis for particles yields a corresponding outcome.

Clauser et al deduced a general rule that locally real hidden variable theories that exhibit enhancement are not subject to Bell's Theorem. [345] However, this exclusion was not considered to be a viable loophole for locally HVT's because the property of enhancement was conjectured to be an implausible physical property, i.e. transmitting a photon through a polarizer plausibly should not increase its transmission through a subsequent, randomly oriented polarizer. [102]-C As a counterexample to this conjecture, enhancement does occur as a natural and plausible property of LR. This does not constitute a conundrum with regard to Bell's Theorem and LR since we can conclude that it is the conjecture itself that is incorrect and Bell's Theorem is not applicable to LR, which is a special case of the class of HVT's that exhibit enhancement.

Because of the flawed conjecture that all physically viable HVT's had the property of non-enhancement, the reported Bell experiments in conjunction with Bell's Theorem have effectively led to the general perception that the entire class of HVT's has been disproved. A consequent corollary to this perception is that pairs of photons (or particles) that exhibit the characteristic quantum correlation are automatically inferred to be non-locally entangled.

It can be appreciated that the scope of LR presented in [102]-C was confined to a treatment of locally real 'observable' states of photons and of particles, i.e. wave structures on which the particle-like quanta reside. This treatment of observable states was certainly sufficient for the principal phenomenon examined in [102]-C, namely demonstrating that Bell Theorem and Bell (EPR) experiments do not exclude LR. [102]-C also treats Malus's law within the boundaries of that restriction.

Here we expand the scope of the [102]-C LR representation in order to encompass a broader class of PI phenomena such as non-local quantum superposition and to provide a more complete representation of local realism. That more inclusive representation is still designated here as LR.

In this more inclusive LR we deduce the states of occupied wave packets and of the associated empty wave packets. The wave functions for these

states are detailed for photons transiting a calcite loop and a M-Z PBS loop and for particles transiting a Stern-Gerlach magnet.

The more inclusive representation of LR presented here also provides critical insights into the associated representation of coherent photon beams at macroscopic powers and is significant since it predicts readily testable consequences of LR that violate PI.

1.2 CONSEQUENCES OF LR AS AN HVT

LR is appropriately classifiable by widely accepted criteria as a “hidden variable theory” (HVT) or more precisely, a locally real hidden variable theory. The characterization that the variable facilitating local realism is “hidden” is misleading in the case of LR. However, as this is an issue of semantics, we defer further examination of that characterization for the present.

LR is fully consistent with the underlying mathematical quantum mechanical formalism. As a comprehensive theory LR may be regarded as locally real interpretation of that formalism. However, LR is distinctly in conflict with the widely accepted Probabilistic Interpretation (PI) of the quantum mechanical formalism. (PI is alternatively identified as the Copenhagen Interpretation.)

The appropriate classification of LR is important because of Bell’s Theorem and results of performed Bell experiments which together purportedly imply that the entire class of locally real HVT’s has been falsified.

An inspection of LR shows that while it is an HVT, it’s derivation from first principles [102]-C naturally incorporates the property of “enhancement” onto so-called correlated pairs of photons and pairs of particles that are employed in Bell experiments. For example, a given correlated photon may have some probability of triggering a measurement by a detector. If that process is repeated, but with a polarizer interposed in the path of that same photon, LR predicts that the probability of triggering a measurement by the detector may increase, i.e. may be enhanced. For LR that probability increase results in exact agreement with performed Bell experiments.

The enhancement property is understandably counterintuitive. An interposed polarizer is expected to reduce the detection probability or at least to leave

that probability unaltered. Accordingly, HVT's with the property of enhancement are generally dismissed as physically implausible.

Clauser and Horne [345] showed theoretically that HVT's with the property of enhancement are not subject to Bell's Theorem. Because of the generally perceived implausibility of the enhancement process, HVT's with the enhancement property are dismissed out of hand while the HVT's without enhancement are falsified by the results of Bell experiments. Accordingly, any Bell test result consistent with PI is commonly regarded as evidence of the non-local phenomenon of entanglement. Such a result is similarly accepted as a falsification of all HVT's.

However, for LR which is not subject to Bell's Theorem, there is a plausible basis for its inherent property of enhancement. In LR a correlated photon transiting a polarizer emerges from a polarizer with, on average, an increased wave packet arc span in the transverse plane physically constituting an increased interaction cross section that results in proportionately increased probability of detection. In that process LR yields outcomes consistent with both the underlying quantum mechanical formalism and with local realism.

It can be appreciated from the foregoing that the "hidden variables" present in LR are not actually hidden. The variables are manifested in the "complete" 3-dimensional LR representation of the wave function itself. That complete representation arises naturally from the derivation of LR. For example, for a photon the critical LR variables resolve to the objectively real transverse arc span and bisector orientation of the standard longitudinal formulation of the wave packet. For particles, the standard formulation of the wave packet is constituted from a coherence wave of spin structures where the complementary particle LR variables are the solid angle and polar orientation of those spin structures.

The representation of particles in LR is closely analogous to that of photons despite the substantial differences in their respective wave structures and the methods used in their measurement. In large part, the analogies arise from mathematical homologies of their respective projective condensation and emission processes.

In the LR representation waves and the particle-like quanta residing on those waves are objectively real. Similarly, properties such as electromagnetic

wave arc bisector orientations and spin structure polar orientations are objectively real. In general, processes that induce projective condensation of the wave structure are deterministic while solitary emission processes are locally mediated by an ensemble distribution of outcomes. Non-local superposition states and entanglements do not exist. Interactions are locally real and fully consistent with relativity. Bell test correlations of separated entities are determined before those entities are separated.

1.3 EMPTY WAVES

The very existence of empty waves of electromagnetic radiation has been the subject of extensive controversy for nearly a century. The principal origin of this controversy relates to various phenomena in which the path of a beam of discrete photons is split and subsequently rejoined. The physical configurations associated with these phenomena include two slit interference, a Mach-Zehnder (MZ) interferometer, a polarizing beam splitter (PBS) MZ interferometer, and birefringent crystal (typically calcite) loops as shown respectively in Figs. 1.1a-d.

For all of these apparatus configurations when both of the two split paths are unobstructed, an interferometric phenomenon is readily observed at the rejoined paths. However, when one of the paths is obstructed, the interferometric phenomenon vanishes based upon the collective outcomes of the discrete photons observed at the location of the recombined paths.

An early interpretation of such divergent results postulated by de Broglie (ref) contends that the discrete photons are each comprised of real wave-like entity and a real particle-like energy entity. In configurations such as those depicted in Figs. 1.1a-d, presumptively the wave-like entity is split onto the two paths and the real energy entity exists on only one path.

In the latter part of the 1920's the advent of "the probabilistic interpretation of quantum mechanics" (PI) became the dominant interpretation and effectively displaced reality-based interpretations, such as that of de Broglie.

For interferometric phenomena, PI postulates that discrete photons exist as probabilistic non-real entities that are simultaneously on both separated paths in a "superposition" state for configurations such as those in Figs. 1.1a-

d. Such photons exhibit either particle-like or wave-like properties depending upon the type of measurement applied to observe them. If an obstruction is placed along one path, a particle-like energy measurement of a photon colliding with that obstruction is associated with a simultaneous, effectively “non-local,” collapse of the

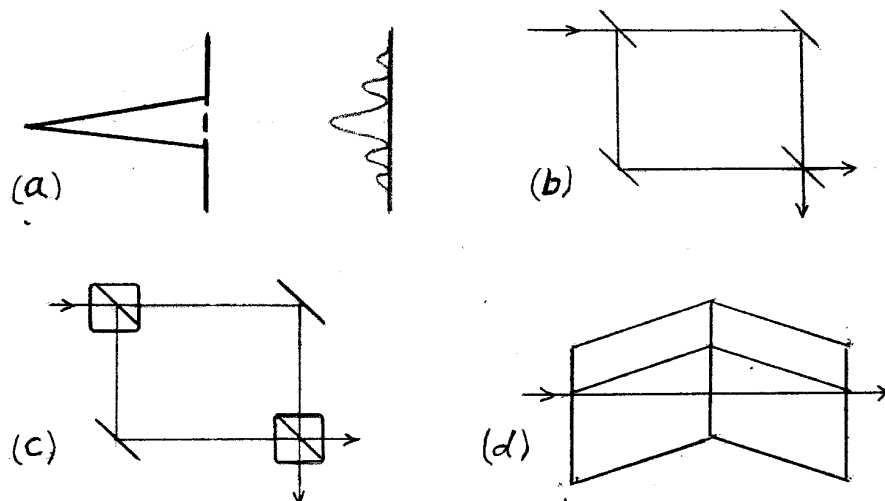


Fig. 1.1a-d. Interferometric configurations.

probabilistic wave-like property of that photon on the other path. Consistent with PI, the measurement of the probabilistic photon at the obstruction instantly requires that the photon have a zero probability of existence on the other path which includes any persistent existence as an empty wave.

In the intervening years since the formulation of PI, indirect support for that interpretation of quantum mechanics has been provided by multiple experiments failing to definitively demonstrate evidence of any such persistent discrete photon empty waves (refs). Most notably however, the broadest level of support for PI is derived from Bell’s Theorem [329] and reported “Bell” experiments concerning pairs of correlated photons as well as correlated particles. [332] [338]

1.4 THE LR REPRESENTATION OF LOCAL REALISM

The LR representation presents an alternative to PI that returns in part to de Broglie’s hypothesis [349] that a photon exists as a real wave entity that can

be split or divided by various means onto two spatially separate paths and a real energy quantum that accompanies the wave entity on only one path leaving a real empty wave on the other path.

Consistent with that de Broglie hypothesis, the wave packet of a photon incident on a common 50:50 beam splitter is divided into two wave packets, each of which is physically identical to the incident wave packet but with half the wave intensity. In the following, quantities relating to the incident photon are identified by an “i” subscript. Similarly, “t” and “r” subscripts respectively identify the transmitted and reflected output wave packets.

Upon exiting the beam splitter, the energy quantum is statistically guided onto one of the two output wave packets based upon their relative intensities. Since those intensities are equal in the present example, there is a 50% random likelihood for any incident photon that the outgoing energy quantum will be guided onto one particular output of the beam splitter resulting in a “photon” comprised a wave packet that has half the intensity of the incident wave packet occupied by an energy quantum. In that event, the other output necessarily yields an “empty” half-intensity wave packet that is unoccupied by an energy quantum.

A single such event can be represented specifically in the nomenclature of the LR representation detailed here. The wave packet of the incident photon can be assigned a unit-less, normalized wave intensity (a probability flux-density) $W_i=1$. Since a single energy quantum resides on that wave packet, the irradiance (an energy flux-density) can similarly be assigned a unit-less, normalized $I_i=1$. The output wave packets have intensities $W_t=W_r=0.5$. If the outgoing energy quantum happens to occupy the transmitted wave packet, $I_t=1$ and, necessarily, $I_r=0$. A parameter denoted as an “occupation value” Ω is introduced here. Ω is a measure of the relative energy quantity occupying a wave structure. In the present example applying the I and W variables, $\Omega_i=I_i/W_i=1$, $\Omega_t=2$ and $\Omega_r=0$. The incident photon with an $\Omega_i=1$ is identified as “ordinary”.

Photons are commonly generated with a fixed proportionality of complementary energy-like and wave-like parameters such as irradiance and intensity, respectively. Accordingly for those photons, normalization of the complementary parameters results in those photons being in an “ordinary” $\Omega=1$ state. The fundamental PI principle of “duality” requires that

this fixed proportionality be universal for all photons and must remain fixed. However, for a representation consistent with de Broglie's hypothesis and the presently considered LR representation, an ordinary state can be altered by interaction with a device such as a beam splitter. That process is appropriately identified here as "duality modulation". From the perspective of LR, both outputs of the beam splitter are duality modulated. In the present example, with respect to resident energy, the transmitted wave packet, which because of its energy quantum constitutes a photon, is "enriched" whereas the reflected wave packet is "depleted", or more precisely, totally depleted since it is empty.

From the perspective of de Broglie's hypothesis and LR, the beam splitter does provide a source of totally depleted, empty wave packets from either output. However, those empty wave packets statistically are accompanied with an equal number of enriched photons and the simple beam splitter does not by itself provide a pure source of empty wave packets.

That deficiency can be remedied by augmenting the beam splitter with more elaborate components configured to separate those empty wave packets from the enriched photons. For example, if a beam of incident discrete photons is very weak and the photons are sufficiently separated longitudinally on that beam, a detector proximal to one output of the beam splitter can be used to generate a brief signal whenever an energy quantum is measured. An electronic gate distal to the beam splitter on the second output is normally closed, blocking passage of photons and empty wave packets as well except when a signal from the detector, heralding the measurement of a photon, briefly opens the gate and permits passage of the empty wave packet associated with that measured photon.

This and other related methods have provided the means for generating and studying presumptively real empty wave packets within the limits of a representation such as that prescribed by the de Broglie hypothesis.

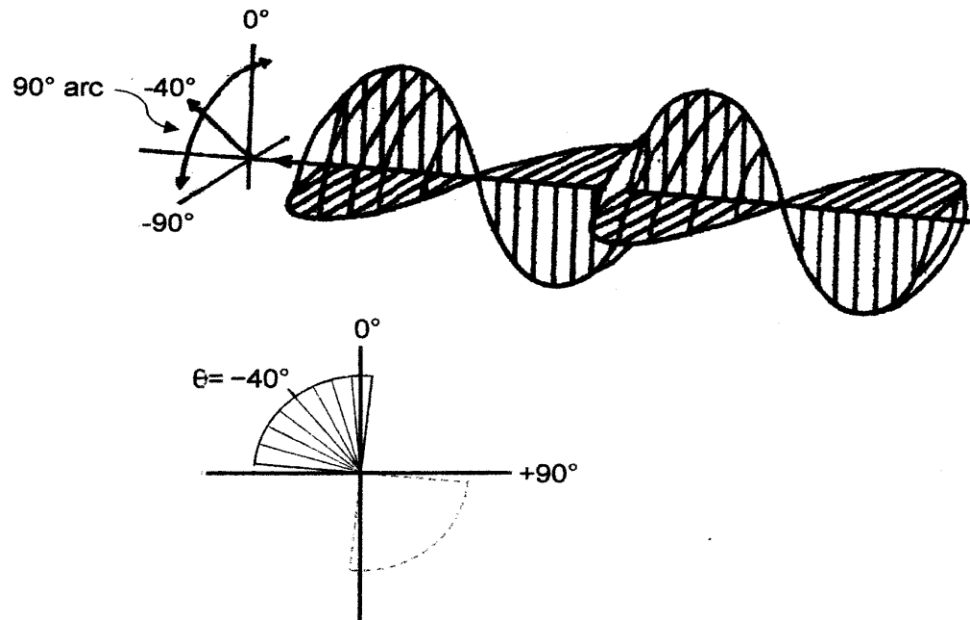


Fig. 1.2. A 3-dimensional depiction of a two-wavelength long segment of a coherent wave and a 2-dimensional cross section of that segment. In the transverse plane the wave's arc bisector at θ defines the orientation of the wave.

However, these methods place restrictive limits on the incident beam, and require fast-operating ancillary electronic components. Historically, these methods have yielded inconclusive evidence for the detection of the presumptively empty waves. More effective methods for generating empty wave packets require the deduction of the transverse aspect of the quantum mechanical wave function.

The principal objective of the LR [102]-C representation is the derivation of a locally real transverse representation of the quantum wave function from first principles that complements the longitudinal representation of the wave function of the underlying mathematical quantum mechanical formalism. (That underlying formalism is distinct from the probabilistic interpretation of that formalism.) The LR representation is shown in [102]-C to be independent of Bell's Theorem. As a consequence, the results of the related "Bell" experiments do not invalidate the LR representation.

With respect to the LR representation of the transverse aspect of the wave function, a typical discrete linearly polarized photon has an objectively real

wave packet that subtends a 90° arc in the plane transverse to the photon's propagation axis as shown in Fig. 1.2. The longitudinal aspect of the wave packet retains the familiar sinusoidal wave structure of the standard underlying quantum mechanical formalism. Fig. 1.2 is a three-dimensional view showing only a short two-wavelength long segment of the entire wave packet. That view shows the longitudinal aspect of the standard formalism together with the LR transverse aspect.

A real energy quantum resides and migrates on the wave packet. As the wave packet propagates past a given point, the arc bisector remains oriented at some fixed angle θ . That θ orientation is equivalent $\theta+180^\circ$ because of the bilateral symmetry of the wave as the longitudinal aspect propagates.

LR [102]-C describes the interaction of that photon with a common one-channel polarizer. The polarization axis of the polarizer is defined to be at 0° . A photon oriented at some random θ has a 50% chance that its wave packet arc will intersect the polarizer axis. When that intersection does occur, the wave transversely condenses onto the inclusive polarizer axis and continues to propagate within the polarizer as a planar wave. In that process, the resident energy quantum is trapped onto the transversely condensing wave and continues propagation within the polarizer as a planar wave photon.

When the planar wave photon reaches the exit face of the one-channel polarizer a "conventional" photon with a 90° arc is emitted. That photon has a random "polarization ensemble" orientation θ' . A large number of photons exiting a linear polarizer constitute members of a polarization ensemble. The relative distribution of ensemble member orientations is given by $\cos^2\theta'$ where the polarizer axis from which it is emitted is defined as 0° . This distribution is derived from first principles in [102]-C.

Fig. 1.3 depicts a crude 16-member approximation of a 0° vertically polarized ensemble. In principle an infinite number of members is required to precisely represent a polarization ensemble. However, a crude finite-member ensemble is highly instructive in considering the phenomenon of linearly polarized photons interacting with a polarizer from an LR perspective. Cosine squared curvilinear boundaries define the left and right boundaries of the Fig. 1.3 ensemble distribution. Each horizontal row identifies the transverse 90° wave arc of a particular representative member. The dot in the middle of a row identifies the orientation of that particular member.

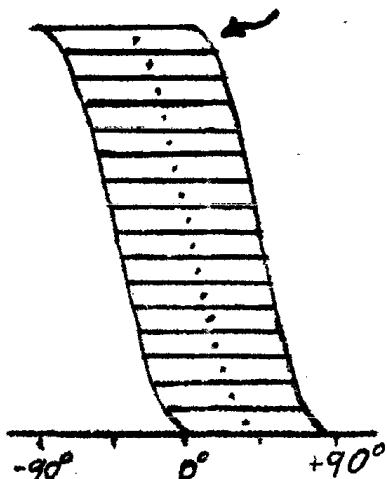


Fig. 1.3. *A 16-member approximation of a polarization ensemble.*

The Fig. 1.3 distribution can be used to represent the ensemble members emitted from the vertical axis output of a 0° -oriented polarizer where the distribution of ensemble member orientations is given by $\cos^2\theta'$. This distribution is verified by considering the outcome of having the axis of a subsequent polarizer oriented at some θ' . If $\theta'=0$, the transverse wave packet arcs of all 16 members are intercepted and all 16 members are transmitted as photons. If $\theta'=60^\circ$, the four member arcs farthest to the right are intercepted and those four members are transmitted as photons by the subsequent polarizer ($\cos^2 60^\circ=0.25$). In general, a $\cos^2\theta'$ fraction of the members is transmitted as photons by the subsequent polarizer in agreement with Malus's Law.

Fig. 1.2 depict arcs with bisectors oriented at -40° . Those arcs then extend from -85° to $+5^\circ$ and would barely be intercepted by a subsequent polarizer axis oriented at $\theta'=0^\circ$. Accordingly, the wave packet arcs depicted in these two figures can be approximately represented by the Fig. 1.3 left-most member arc indicated by an arrow.

Statistically, 50% of totally randomly oriented photons incident on some particular polarizer will not have their respective wave packets intersect that polarizer's axis. For any of those photons, the energy quantum is still trapped on the photon's condensing wave packet as it enters the polarizer, however,

no planar propagation route is available to the energy quantum and its energy is absorbed by the polarizer.

1.5 EMPTY WAVES

The above LR [102]-C representation of photon interactions with polarizers accurately treats the measurement outcomes of the readily detectable energy quanta residing on incident photons. In order to deduce a productive mechanism for generating empty waves, that LR [102]-C representation must be generalized. In this regard we consider linearly polarized photons incident on a two-channel polarizer such as a birefringent calcite crystal.

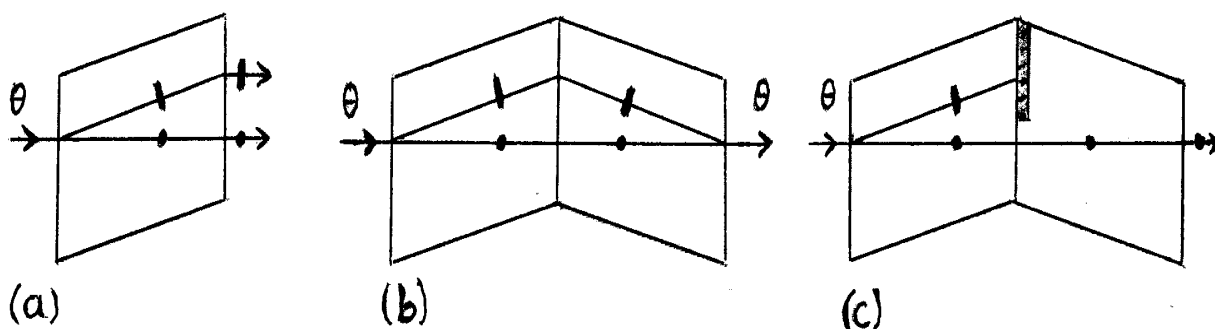


Figure 1.4a-c. In (a), an incident photon oriented at a particular angle, may be emitted from a calcite polarizer as a vertically polarized photon at the vertical axis output or as a horizontally polarized photon at the horizontal axis output depending upon the value of that particular angle. For (b) a calcite loop, the output photon replicates the incident photon whereas for (c) an unaccompanied vertically oriented planar photon at the exit face of the loop produces a vertically polarized output photon with an orientation that is uncorrelated to that of the incident photon.

Fig. 1.4a is a plane view of a calcite crystal. The depicted rhombus shape corresponds to the natural cleavage planes of calcite. A beam of linearly polarized photons is incident on the left, normal to the calcite surface. Each of these incident photons is linearly polarized but has a random orientation θ independent of that of the other photons. In that Fig.1.4a configuration, one of the two polarization axes of the calcite is perpendicular to the figure plane. That axis can be defined to be “vertical” and oriented at 0° . The other

polarization axis is defined as “horizontal”, is oriented at 90° and lies in the plane of the figure.

If an incident photon’s arc bisector orientation is within $\pm 45^\circ$ of 0° , its arc intersects the vertical polarization axis of the calcite. As a result, a planar wave photon propagates on the calcite’s vertical axis channel path identified by a solid dot in Fig. 1.4a. That planar wave photon exits from the vertical channel of the calcite as a random member of a vertically polarized ensemble with a bisector orientation uncorrelated to that of the incident photon.

Similarly, if an incident photon’s arc bisector orientation is within $\pm 45^\circ$ of 90° , its arc intersects the horizontal polarization axis of the calcite and a planar wave photon propagates on the calcite’s horizontal axis channel path identified by a short solid line. That planar wave photon exits from the horizontal channel of the calcite as a random member of a horizontally polarized ensemble with a bisector orientation uncorrelated to that of the incident photon.

In either case, only one channel of the calcite is occupied by a “photon” (a wave packet accompanied by an energy quantum), but no insight is gained regarding the channel without the energy quantum. That insight, from the perspective of LR, can be deduced by examining a “calcite loop” depicted in Fig. 1.4b. A linearly polarized photon with its arc bisector oriented at some angle θ is known to be exactly replicated upon transmission through the loop. The process is quantum mechanically identified as “unitary.”

For consistency with LR, this unitary process requires the projection of the incident wave amplitude onto the vertical and the horizontal axes of the first calcite. For example, if the incident photons are all “vertically polarized,” any of those photons is a random member of a 0° polarization ensemble. Any particular member has an objectively real orientation θ that is within $\pm 45^\circ$ of the first calcite vertical polarization axis at 0° . If each incident photon is assigned a unit amplitude represented as a unit vector of the arc bisector, the projected amplitudes onto the first calcite vertical axis and the horizontal axis are reduced respectively by factors $\cos \theta$ and $\sin \theta$, respectively.

In the first calcite, that amplitude projection results in a planar wave packet on the vertical channel accompanied by the energy quantum that had been on the incident photon. On the horizontal polarization channel there is also a

planar wave packet, but that wave packet is unaccompanied by an energy quantum.

That horizontally oriented planar wave packet in the first calcite constitutes a real empty wave essentially extracted from the incident photon. The possible negative sign on the amplitude introduced by the $\sin \theta$ factor when the incident photon orientation $\theta < 0^\circ$ merely indicates a π phase shift of the longitudinal planar wave packet relative to its phase if instead $\theta > 0^\circ$. In the present consideration of discrete vertically polarized photons, that phase shift is not of consequence.

The reality of the empty planar wave packets in the horizontal channel from the perspective of LR may be appreciated when analyzing outcomes with the contiguous second calcite completing the Fig. 1.4b calcite loop. That second calcite loop efficiently couples respective vertical and horizontal channels of both calcites. The “reversed” orientation of the second calcite combines the vertical and horizontal planar wave packets at the exit face of the loop. The vectorial resultant of this combination is an amplitude oriented at the same θ as that of the incident photon and the calcite loop emits a conventional 90° arc span photon with an orientation θ identical to that of the incident photon.

The projections of real waves onto the vertical and horizontal axes of the calcite loop are superficially reminiscent of the PI superposition of probabilistic non-real photon waves on those axes. However, the clear distinction imposed by LR [102]-C is that the incident photon has an objectively real orientation θ of its 90° arc that deterministically fixes the energy quantum only onto the axis intercepting the arc.

If the second calcite of the loop has a blocked horizontal channel as depicted in Fig. 1.4c, the vertical planar wave packet arrives at the exit face of the second calcite unaccompanied by a horizontal wave packet. If for a particular incident photon the energy quantum is present on the vertical planar wave packet, a vertically polarized photon is emitted from the loop. The orientation θ' of that emitted photon is not in general identical to the orientation θ of the incident photon. That θ' is the orientation of a random member of a vertical polarization ensemble.

1.6 BASIS FOR THE EXISTENCE OF EMPTY WAVES

This section provides a comprehensive self-contained but brief summary of the basis for demonstrating the existence of objectively real empty waves which is central to a complete LR formulation of local realism. The basis utilizes specific properties of photons predicted by LR and is consistent with the underlying formalism of quantum mechanics and performed Bell experiments.[102]-C The subject matter of this single 1.6 BASIS section is covered in more detail together with extensive related matters in the multiple subsequent sections below.

Fig. 1.2 depicts a short section of the objectively real 3-dimensional structure of an “ordinary” photon wave packet propagating in free space. An energy quantum residing on that wave packet is not depicted. The Fig. 1.2 cross section of that structure shows in greater detail a sampling of the wave packet’s constituent radial vector amplitudes that span a 90° arc in the transverse plane. The respective constituent radial vector amplitudes in any particular wave packet cross section are equal in amplitude magnitude. In the example depicted in Fig. 1.2 the wave packet arc happens to intersect the “vertical” axis defined as 0° . (In general, photons are “ordinary” with 90° arc spans. However, one member of a correlated photon pair is typically non-ordinary in the regard that it has a $<90^\circ$ arc span.)

The squared magnitude of a constituent vector amplitude at a point along the wave packet represents the wave intensity at that point and the spatial integral of the wave intensity over the entire wave packet represents the wave packet’s probability P . (In LR “probability” refers to an objectively real integrated wave intensity and is distinct from the extended use of that term in the probabilistic interpretation of quantum mechanics (PI) in denoting non-real and non-local entities, e.g. “probability waves”.) The opposed dashed-line perimeter depicts the cross section that is half a wavelength distal along the propagation path. Each constituent amplitude in the Fig. 1.2 cross section is associated with a longitudinal wave mathematically represented by the underlying quantum mechanical formalism and spatially constitutes a planar-like wave at the transverse orientation of that constituent amplitude. These planar-like waves are contiguous and collectively comprise the 90° arc of the 3-dimensional structure. The arc bisector is oriented at some θ in the transverse plane. In Fig. 1.2, $\theta = -40^\circ$.

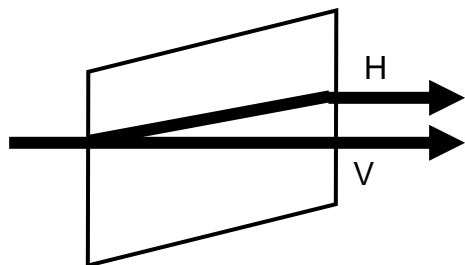


Fig. 1.5. Photon wave incident on a 2-channel calcite polarizer. The objectively real wave has an arc bisector orientation at some θ in the plane transverse to the incident wave. The wave amplitude is projectively split onto the calcite's vertical polarization axis and horizontal polarization axis. The vertical polarization axis is normal to the plane of the figure. V and H denote the separate channels on which the two objectively real projections respectively propagate.

We now examine the process of photons incident on a 2-channel polarizer such as a calcite crystal shown in Fig. 1.5. The vertical polarization axis is normal to the plane of the figure. The probabilities of all incident photon wave packets are normalized to unity, $P=1$. Because of the 90° arc spans only one of the polarizer's polarizations axes is intersected by any incident wave packet. If the presently considered photon with $\theta=-40^\circ$ is incident, the polarizer's vertical axis is intersected. As cross sections of the wave packet progressively enter the polarizer, the constituent amplitudes within that cross section projectively condense along that intersected V axis.

The projective condensation process is the physical realization of the formation of a Dirac-delta function. Each constituent amplitude contributes to the total axial projection its magnitude reduced by the cosine of the angle between that amplitude and the axis. Notably, because of the radial geometry of those constituent amplitudes, the resultant axial vector amplitude along the V axis has a magnitude that reduces to $\cos \theta$ times the sum of those constituent amplitude magnitudes. The atomic structure of the calcite polarizer confines the propagation of the resultant V axial vector amplitude to the V -channel path within the polarizer. In this process, the incident 3-dimensional wave packet is effectively reduced to a 2-dimensional planar wave packet propagating within the polarizer, transversely

represented by the V axial vector amplitude depicted in the Fig. 1.5a cross section.

As an important ancillary matter, the energy quantum that had resided at some point on the incident wave packet is effectively trapped onto the V axial vector as the constituent vector amplitudes on which the energy quantum locally resides enter the polarizer and projectively condense onto the vertical polarization axis. Consequently, in the present case of $\theta = -40^\circ$, the Fig. 1.5a vertically oriented planar wave packet propagating on the vertical channel of the polarizer is appropriately identified as a photon in the regard that it is an “occupied” wave packet comprised of both a wave packet and an energy quantum.

When that V channel (occupied) planar wave packet reaches the exit face of the polarizer, the projective condensation process that had occurred at the incident face of the polarizer is substantially reversed. At the exit face of the polarizer the V-channel output emits a 3-dimensional (occupied) wave packet that has an orientation θ' (uncorrelated to θ) that is appropriately identified as a “vertically polarized wave packet” (that happens to be occupied). The cross section of that emitted photon is shown in Fig. 1.5b.

In the context of LR, a vertically polarized wave packet has an objectively real orientation θ' where $-45^\circ < \theta' < 45^\circ$ (or equivalently $135^\circ < \theta' < 225^\circ$) since the wave packet is emitted from a vertical polarization channel. The value of that θ' can be statistically predicted. A sufficiently large sampling of photon wave packets polarized along a particular axis constitutes the wave packet “members” of a “polarization ensemble” associated with that axis. (This characterization of ensemble members applies whether or not the wave packets are occupied, i.e. are photons.) The individual members are identifiable by their respective θ' orientations. Over the ensemble distribution, the density of θ' orientations peaks at the orientation of the polarization axis and monotonically decreases to zero at $\pm 45^\circ$ from that axis. For the presently considered case of a vertical axis polarization ensemble the distribution of θ' is functionally given by $F_V(\theta') = \cos 2\theta'$. Consequently, any wave packet emitted from the vertical output of the polarizer statistically has the orientation of a random member of the vertical polarization ensemble.

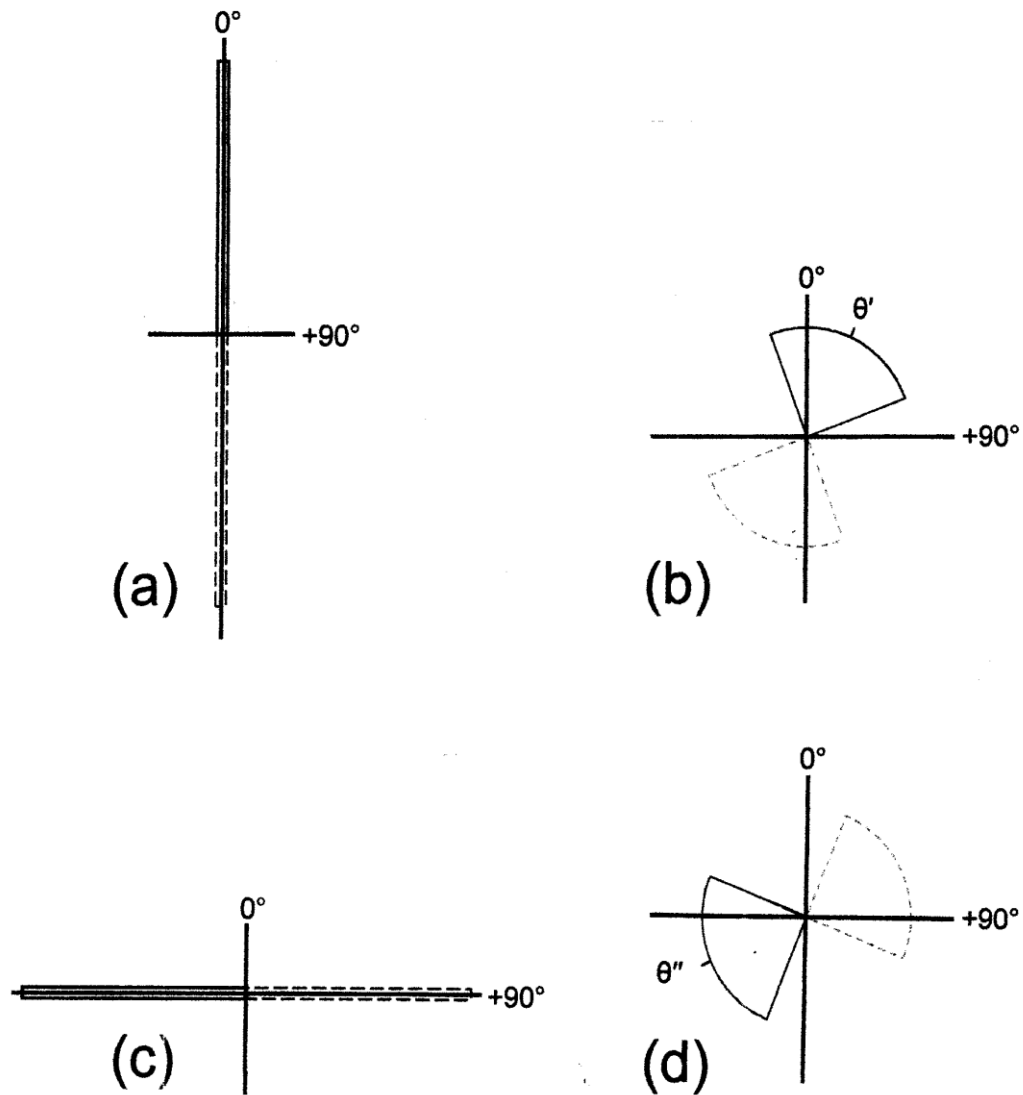


Fig. 1.5a-d. Transverse cross sectional representations of waves propagating within the calcite polarizer and after exiting the calcite polarizer. (a) shows the cross section of the V-channel planar wave propagating within the polarizer confined as Dirac-delta amplitude along the vertical polarization axis. (b) depicts the cross section of a V-channel wave after exiting. (c) and (d) are complementary H-channel representations.

The vertical output wave packets also have a deterministic property related to the orientation of the incident photon's wave packet from which they were derived. In the case of the particular vertical output photon initially derived from an incident $P=1$ photon oriented at $\theta=-40^\circ$, we noted that the axial projection of the constituent amplitudes onto the polarizer's vertical axis is reduced by the cosine of the bisector orientation which in the present case is $\cos \theta = \cos -40^\circ = 0.766$. This reduction has important implications for the 3-dimensional vertically polarized wave packet that emerges from the exit face of the polarizer.

The magnitudes of the 3-dimensional wave packet constituent amplitudes that progressively emerge from the polarizer are derived in equal measure from the magnitude of instantaneous axial projection amplitude that had arrived at the polarizer exit face. Because of the 0.766 amplitude reduction factor of the axial projection amplitude that occurred at the incident face, the emerging constituent amplitudes are also reduced by that 0.766 factor at points along the wave packet relative to constituent amplitudes at corresponding points along the incident wave packet. As a result, the wave intensity at points along the emergent wave packet are reduced by a factor $(0.766)^2 = 0.587$ relative to corresponding points along the incident wave packet. Consequently, the integral of intensity over that emergent wave packet yields a $P_V(-40^\circ) = 0.587$. In that process a $P=0.413$ is missing from the emergent (occupied) wave packet relative to the incident photon's $P=1$.

This example can be generalized. For any incident photon oriented at θ where $-45^\circ < \theta < 45^\circ$, an occupied wave packet, i.e. a photon, will emerge from the polarizer with the orientation θ' of a random member of a vertical polarization ensemble and will have $P_V(\theta) = \cos^2 \theta$ independent of that θ' . This initial condition of incident photons oriented in the range $-45^\circ < \theta < 45^\circ$ is readily provided by using a source that generates vertically polarized photons. Use of such a source is advantageous since all of the photons incident on the polarizer result in a photon being emitted from the vertical channel output.

In the above process a second projection phenomenon occurs as photons are incident on the polarizer. We again follow the example of the $\theta=-40^\circ$ incident photon since the results are readily generalized to any θ where $-45^\circ < \theta < 45^\circ$. As the incident photon enters the polarizer, the projective

condensation of the constituent amplitudes onto the vertical polarization axis is accompanied by a projection onto the orthogonal horizontal axis.

In analogy to the vertical axis projection, the horizontal axis projection of the constituent amplitudes resolves to a resultant axial vector amplitude along the polarizer's H axis with a magnitude that is $\sin \theta$ times the sum of the constituent amplitude magnitudes. This H axis projection differs from that of the V axis because the H axis does not intersect the incident wave packet arc of constituent amplitudes oriented at $\theta = -40^\circ$. As a result, the energy quantum is not acquired onto the H axial vector amplitude.

The H axis projection further differs from that of the V axis because of the $\sin \theta$ factor which introduces a positive sign for incident $\theta > 0^\circ$ and a negative sign for $\theta < 0^\circ$. The sign differential merely signifies a π phase shift of the H axial vector amplitude relative to incident $\theta > 0^\circ$ photons as opposed to $\theta < 0^\circ$ photons.

In analogy to the V axial vector amplitude the H axial vector amplitude analogously propagates in the polarizer as a planar wave packet but as an empty planar wave packet transversely confined by the atomic structure of the polarizer to a $\pm 90^\circ$ orientation on a refracted H-channel path as shown in the Fig. 1.5c cross section of that planar wave packet. (Because of the refracted H-channel path, the Fig. 1.5c $\pm 90^\circ$ propagation axis is not parallel to the Fig. 1.5a $\pm 90^\circ$ axis.)

When the empty planar wave packet reaches the exit face of the polarizer, the H-channel output emits a 3-dimensional empty wave packet that has an orientation θ'' (uncorrelated to θ and θ'). The output empty wave packet depicted in the Fig. 1.5d cross section is horizontally polarized and has an objectively real orientation θ'' where $45^\circ < \theta'' < 135^\circ$ (or equivalently $225^\circ < \theta'' < 315^\circ$) since it is emitted from a horizontal polarization channel.

As with the θ' value of the emitted vertically polarized occupied photon, the value of θ'' for the emitted empty wave packet can also be statistically predicted. For the horizontally empty wave packet the distribution of θ'' is functionally given by $F(\theta'') = \cos [2(\theta'' - 90^\circ)]$ and has the orientation of a random member of a horizontal polarization axis ensemble.

The horizontally polarized output empty wave packets also have a deterministic property related to the orientation of the incident photon from

which they were derived. In the case of the particular horizontal output empty wave packet derived from an incident $P=1$ photon oriented at $\theta=-40^\circ$, the horizontal axis projection of the constituent amplitudes resolves to a resultant axial vector amplitude along the H axis with a magnitude that is $\sin \theta$ times the sum of the constituent amplitude magnitudes which in the present case is $\sin \theta = \sin -40^\circ = -0.643$. As noted above the negative sign merely signifies a π phase shift of the planar empty wave packets relative to incident $\theta > 0^\circ$ photons as opposed to $\theta < 0^\circ$ photons. That phase shift distinction also applies to the output empty wave packets. In the context of discrete incident photons that phase shift is not consequential.

When the planar wave packet reaches the output face of the polarizer, all of the constituent amplitudes of the 3-dimensional wave packet that emerge from the polarizer are reduced by that 0.643 factor relative to the corresponding constituent amplitudes of the incident photon wave packet independent of the θ'' orientation of the emergent wave packet. As a result, that emergent empty wave packet also has a wave intensity reduced by a factor $(0.643)^2 = 0.413$. Consequently, the integral of intensity over that emergent wave packet yields a $P_H(-40^\circ) = 0.413$. In that process the $P = 0.413$ missing from the emergent photon relative to the incident photon's $P = 1$ is identified.

This empty wave packet example can be generalized. For any incident photon oriented at θ where $-45^\circ < \theta < 45^\circ$, an empty wave packet will emerge from the polarizer with the orientation θ'' of a random member of a horizontal polarization ensemble and will have a $P_H(\theta) = \sin^2 \theta$ independent of that θ'' . If the initial condition of incident photons oriented in the range $-45^\circ < \theta < 45^\circ$ is provided by using a source that generates vertically polarized photons, empty wave packets are then emitted exclusively from the H channel output.

From the above we see that the probabilities of the emergent occupied and empty wave packets, $P_V(\theta) = \cos^2 \theta$ and $P_H(\theta) = \sin^2 \theta$ respectively, are independent of their orientations θ' and θ'' , respectively, and are deterministic with respect to the orientation θ of the incident photon wave packet from which they are derived. If the source of those incident photons generates vertically polarized photons, the average emergent probability from either channel can be calculated. For the vertically polarized incident photons $F(\theta) = \cos 2\theta$ gives the distribution of ensemble member θ

orientations. Then the integrals of $\cos 2\theta \cdot \cos^2 \theta$ and $\cos 2\theta \cdot \sin^2 \theta$ over $-45^\circ \rightarrow +45^\circ$ respectively give the distribution-weighted probabilities of the V and the H channel emergent wave packets. The average emergent wave packet probabilities are approximately $\langle P_V \rangle \approx 0.89$ and $\langle P_H \rangle \approx 0.11$ (or more precisely 0.8927 and 0.1073, respectively).

In the present context of differentially testing the probabilistic interpretation of quantum mechanics (PI) and the particular representation of locally realism (LR) examined here, the $\langle P_H \rangle \approx 0.11$ value is of particular interest since objectively real empty waves are not consistent with PI. From the perspective of LR the result $\langle P_H \rangle \approx 0.11$ shows that a source of vertically polarized discrete photons incident on a calcite 2-channel polarizer[†] provides a beam consisting exclusively of horizontally polarized empty wave packets that have a probability (integrated wave intensity) that is about 11% of the photon probability from which they were extracted.

From the perspective of LR and other locally real representations, discrete empty wave packets can also be provided by other means such as directing discrete photons at a conventional beam splitter. If a 90:10 beam splitter is used, the output from the $T=0.9$ channel consists of wave packets with $P=0.9$, 90% of which are occupied and 10% of which are empty. Those empty wave packets have probabilities that are nearly as great as the incident $P=1$ photon wave packets from which they are derived and over eight times greater than the average $P \approx 0.11$ from the polarizer which should be a distinct advantage in any method for demonstrating the existence of empty waves. When using a conventional beam splitter, the complication of the photons mixed in with the empty wave packets can be circumvented by monitoring the second beam splitter output with a photon detector to herald a $P=0.9$ empty wave packet at the first output and to briefly open a gate that otherwise blocks that first output. Still other methods for presumptively generating discrete empty wave packets have been examined.

Over many decades a number of ingenious methods have been proposed for determining whether or not empty photon wave packets exist. Some of these proposals have been experimentally tested with outcomes that have variously been inconclusive and controversial however definitive experimental evidence for the detection of these discrete empty wave packets has been elusive. If discrete empty wave packets do in fact exist we

can reasonably surmise that their detectability is below the threshold of widely reported experiments.

The present LR analysis to this point does little in the way of resolving a problem that may be, at its root, an inherently low detectability of discrete empty wave packets. Furthermore, employing discrete empty wave packets with a relatively low average probability $\langle P \rangle \approx 0.11$ would only be expected to exacerbate a problem of low detectability.

The method for investigating the existence of empty wave packets described here avoids that problem. Under LR, “coherent modes” of multiple photons have a wave structure that is closely analogous to that of discrete photon wave packets. In that regard, from the perspective of LR, the 3-dimensional structure depicted in Fig.1.2 is representative of a two-wavelength section of a discrete photon as well as of a coherence mode of photons. This commonality follows from the composition of modes.

Single longitudinal mode (SLM) lasers[‡] provide a convenient source of single mode radiation in the optical regime. An SLM laser emits single modes in succession where the coherence length of each mode contains a huge multitude of energy quanta and has a length that can typically be on the order of ~ 100 m. Those collective quanta relative to the total probability of the coherence length are in the same proportion as the quantum of an ordinary discrete photon relative to the probability of its associated wave packet.

If, additionally, a vertically polarized SLM laser is utilized, each successively emitted coherence length mode has the orientation of a random member of a vertical polarization ensemble of photons (or, more generally, of modes). When that beam is incident on a calcite crystal, the resultant H output beam similarly consists of sequential single longitudinal coherence modes but with a wave intensity (probability flux density) that is on average $\sim 11\%$ as large as that of the incident laser beam and with negligible irradiance (energy flux density). If for example the incident SLM laser beam had a power of 1 Watt, the H output beam would have the macroscopic wave intensity of a horizontally polarized 110 mW laser beam with respect to its wave structure but with virtually no energy quanta. Because photons are bosons, each of the empty output coherence modes constitutes an enormous probability sink for any encountered energy quanta, many orders of magnitude greater than

that of a fractional probability empty wave packet extracted from a discrete photon.

The objectively real existence of the empty horizontally polarized SLM beam is readily demonstrated by transient intersection of that empty wave beam with an ordinary occupied horizontally polarized SLM “restoration” beam of the same wavelength. In the region of beam intersection the energy quanta on the restoration beam equilibrate on the two beams resulting in a net transfer of energy quanta onto the originally empty SLM beam which emerges from that intersection region restored to a conventionally detectable beam.

In contrast, tests for the existence of empty wave packets derived from discrete photons typically require elaborate apparatus and necessitate very exacting criteria in measuring an interaction of a fractional probability wave packet with a discrete photon.

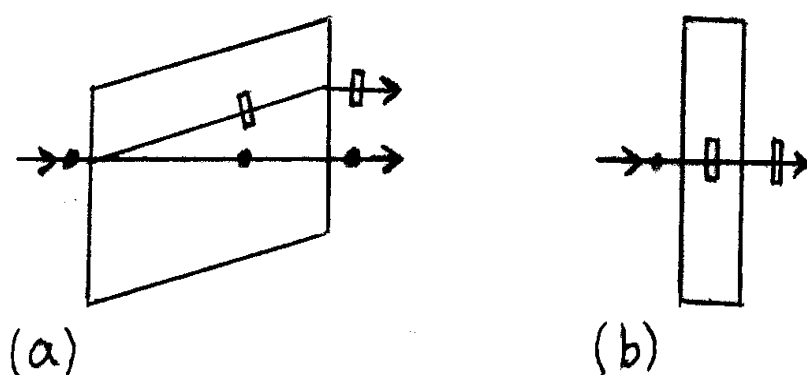
* The underlying principles of this Basis are derived in large part from Reference [102]-C. Further essential principles and methods are detailed in other references such as [209]. See **References**.

†As an ancillary matter, the two channel calcite polarizer can be replaced by a common one channel polarizer rotated to block transmission of the vertically polarized SLM beam for purposes confined to empty waves.

‡Multi longitudinal mode (MLM) lasers, which are less costly and more ubiquitous than SLM lasers are problematic with regard to their use in the demonstration of empty waves. The multiple longitudinal modes that comprise each MLM coherence length respectively have transverse orientations of random members of a polarization ensemble. Then, because of the $\sin \theta$ empty wave projection factor when transiting a polarizer, approximately half of the modes in each coherence length will have a phase shift of π relative to those of the other half. The resultant mutual destructive interference produces a low composite empty wave intensity that suppresses efficient equilibration when intersected with an ordinary MLM photon beam.

1.7 THE GENERALIZED LR LOCAL REALISM REPRESENTATION

From a theoretical perspective, the combination of the [102]-C LR treatment of the energy quanta observables augmented by the inclusion of projections of real wave amplitudes onto polarizer axes provides a generalized representation of local realism which in turn forms the basis for self-consistent representations of phenomena conventionally treated by PI as non-local superposition of non-real probabilistic entities.



Fig's. 1.6a-b. In (a) a two-channel calcite crystal with vertically polarized incident photons provides an output from the horizontal axis that consists of empty wave packets. A one-channel polarizer (b) similarly provides an output of empty wave packets when the polarization of the incident photons is orthogonal to the polarizer's single axis.

That generalized LR representation shows that an incident beam of discrete photons linearly polarized along one axis of a single calcite crystal provides a source of discrete empty wave packets from the output of its other axis. For example, consider that the beam's polarization is aligned with the vertical (0°) axis of the calcite. This condition is explicitly symbolized in Fig. 1.6a by a solid dot on the incident beam on the left which in this case represents that vertically polarized beam of photons. Each photon's orientation is statistically represented by the orientation of a random member of a vertically polarized polarization ensemble (approximately given by Fig. 1.3). Inside the calcite, the solid dot in the context of the calcite's vertical channel path now represents the vertically oriented planar wave packet photons. Those planar wave packet photons arrive unaccompanied at the output face of the calcite (unlike the accompanied output face conditions for a calcite loop Fig. 1.4b).

As a result, the output photons constitute a vertically polarized ensemble with the particular ensemble member orientation of any emitted photon being uncorrelated to the orientation of the incident photon from which it was derived. The process is quantum mechanically characterized as “non-unitary”. In this circumstance the solid dot on the vertical channel output beam once again represents photons of a vertically polarized ensemble.

Since the photons incident on the calcite in this example are explicitly identified as vertically polarized, the real entities on the horizontal polarization channel in the calcite are all empty planar wave packets oriented at 90° (in the plane of the figure) and are unambiguously represented by a short non-solid line. Those empty planar wave packets arrive unaccompanied at the output face of the calcite unlike the accompanied output face conditions for a calcite loop Fig. 1.4b. As a result, the output empty wave packets constitute a horizontally polarized ensemble with the particular ensemble member orientation θ' of any emitted empty wave packet being uncorrelated to the orientation θ of the incident photon from which it was extracted. The process is again quantum mechanically characterized as non-unitary.

Any particular empty wave packet has an amplitude magnitude of $|\sin \theta|$, recalling that all of the incident photons have been assigned unit amplitude magnitudes. The corresponding intensity of that wave packet is given by $W = \sin^2 \theta$. “W” is used here to denote the wave-related parameter that is the squared modulus of a wave amplitude and is explicitly distinct from an energy-related quantity such as the energy flux, irradiance, identified here as “I”.

An analogous process simultaneously occurs on the vertical axis channel of the single calcite for that θ -oriented incident photon aside from the fact that the planar wave packet and the emitted wave packet are occupied by the incident photon’s energy quantum and those wave packets are then both appropriately characterized as “photons.” The wave packet of the emitted photon has an amplitude magnitude $\cos \theta$, an intensity $W = \cos^2 \theta$, and an orientation θ'' that is the orientation of a random member of a vertical (0°) polarization ensemble. That θ'' is uncorrelated to θ and to θ' .

Because the emitted wave packet intensity is generally less than that of the incident photon, the emitted photon is appropriately characterized here as

“energy-enriched” or simply “enriched” in the sense that the full energy quantum resides on a wave packet having a less than unity intensity in contrast to that of the incident photon. Conversely, the empty wave packet emitted by the horizontal channel is appropriately characterized as “totally energy-depleted” or simply “totally depleted.” (LR wave states having enrichment or depletion constitute violations of PI wave-particle duality.)

It is notable that the two intensities, $\cos^2 \theta$ and $\sin^2 \theta$, sum to unity in this representation. Each intensity integrated over the (real) wave packet constitutes the quantum mechanical “probability” in the LR representation. The unit sum of those intensities is an expression of consistency with probability conservation inherent in the underlying quantum mechanical formalism.

From the above considerations, it can be deduced that replacing a two-channel polarizer such as calcite with a one-channel polarizer as depicted in Fig. 1.6b would also provide a comparable source of discrete empty wave packets when the polarizer’s single axis is horizontally oriented. All of the incident photon energy quanta are absorbed in the polarizer but amplitude projection still occurs onto the one-channel polarizer’s single axis thereby generating only empty wave packets from that axis output.